Hindawi Publishing Corporation
Journal of Nanotechnology
Volume 2015, Article ID 727210, 7 pages
http://dx.doi.org/10.1155/2015/727210

Research Article

Synthesis and Application of Magnetic Photocatalyst of Ni-Zn Ferrite/TiO_2 from IC Lead Frame Scraps

Robert Liu and H. T. Ou

Department of Chemical and Materials Engineering, Minghsin University of Science and Technology, Hsinchu 30401, Taiwan

Correspondence should be addressed to Robert Liu; robertl@must.edu.tw

Received 4 June 2015; Accepted 20 August 2015

Academic Editor: Oded Millo

IC lead frame scraps with about 18.01% tin, 34.33% nickel, and 47.66% iron in composition are industrial wastes of IC lead frame production. The amount of thousand tons of frame scraps in Taiwan each year is treated as scrap irons. Ni-Zn ferrites used in high frequent inductors and filters are produced from Ni-Zn ferrite powders by pressing and sintering. The amount of several ten thousand tons of ferrites of $Ni_{1-X}Zn_XFe_2O_4$ in compositions is consumed annually in the whole world. Therefore, these IC lead frame scraps will be used in this research as raw materials to fabricate magnetic ferrite powders and combined subsequently with titanium sulfate and urea to produce magnetic photocatalysts by coprecipitation for effective waste utilization. The prepared Ni-Zn ferrite powder and magnetic photocatalyst (Ni-Zn ferrite/TiO_2) were characterized by ICP, XRF, XRD, EDX, SEM, SQUID, and BET. The photocatalytic activity of synthesized magnetic photocatalysts was tested by FBL dye wastewater degradation. TOC and ADMI measurement for degradation studies were carried out, respectively. Langmuir-Hinshelwood kinetic model of the prepared magnetic TiO_2 proved available for the treatments. Wastes are transformed to valuable magnetic photocatalysts in this research to solve the separation problem of wastewater and TiO_2 photocatalysts by magnetic field.

1. Introduction

Wastewaters from textile and dyeing industries are highly colored by various nonbiodegradable dyes which cause serious environmental problems [1]. Advanced oxidation processes such as UV/H_2O_2 [2], ozonation [3–5], Fenton processes [5–8], ozone/Fenton [9], and TiO_2 and modified TiO_2 [10–17] are promising alternatives for the mineralization of textile dyes or other pollutants. Among them, semiconductor TiO_2's simultaneous photocatalytic oxidation and reduction show significant potential due to being photoreactive, nontoxic, chemically and biologically inert, photostable, and lower in cost. Among different advanced oxidation processes (AOPs), a brand new AOP, sonolysis or hybrid AOP, combined with sonolysis has drawn increasing attention as it generates $^{\cdot}OH$ free radical through transient cavitation by ultrasound irradiation [18–20]. Cavitation is essentially the nucleation, growth, and transient implosive collapse of gas bubbles driven by ultrasound wave.

The well-known nickel-zinc ferrite is of special technological significance, particularly at high frequencies, because of its high resistivity and low eddy current losses. Several methods are conventionally used for the synthesis of these nanosized ferrites such as ceramic [21, 22], sol-gel [23, 24], coprecipitation [25], hydrothermal method [26, 27], citrate precursor method [28, 29], and autocombustion method [29, 30]. Sonochemical approach is considerably new to synthesize ferrite in which ferrite nanoparticles are prepared by ultrasound irradiation or sonication of the reaction mixture [31].

Despite existing technologies, separation difficulty of nanosized TiO_2 particles from treated wastewater still remains. Fixed-film-TiO_2 systems are undermined due to immobility while magnetic TiO_2 offers to overcome this limitation. For example, Chen and Zhao [32] reported a magnetically separable photocatalyst of $TiO_2/SiO_2/\gamma$-Fe_2O_3 prepared by solid phase synthesis. The addition of a SiO_2 membrane between the γ-Fe_2O_3 core and the TiO_2 shell weakened the adverse effects of γ-Fe_2O_3 on the photocatalysis of TiO_2. Photocatalysts in Chen and Zhao's article showed good photocatalytic activity and could be separated from the

solution with magnetic field. Gao et al. [33] synthesized a magnetically separated photocatalyst of TiO_2/γ-Fe_2O_3 by sol-gel method. The sample sintered at 500°C displayed the highest degradation activity for acridine dye aqueous solution, with the optimal TiO_2 supporting amount approximating 50%. Fu et al. [34] successfully prepared TiO_2/NiCuZn ferrite composite powder as a magnetic photocatalyst. The core NiCuZn ferrite powder was synthesized with the waste material from steel and electroplating industries. TiO_2 nanocrystal shell was prepared by sol-gel hydrolysis of titanium isopropoxide with NiCuZn ferrite powder followed by heat treatment. In their study, the optimum dosage of the magnetic photocatalyst was 2.67 g/L to treat methylene blue solution.

Recently we produced MnZn ferrite powders [35], which are used in power transformers and inductors, from spent alkali-manganese batteries in order to solve their heavy metal contamination problem. Comparing with MnZn ferrite, Ni-Zn ferrite is easier to be prepared. Lower temperature and no protecting atmosphere are needed during sintering. Therefore Ni-Zn ferrite was chosen to produce magnetic photocatalysts from IC lead frame scrap and waste pickling acid. Both ferrites solve the different heavy metals pollution problems and transform into useful magnetic photocatalysts.

In this research, a simple magnetic photocatalyst preparation was undertaken. First, Ni-Zn magnetic ferrite powder was prepared from IC lead frame scraps and ferrous sulfate containing spent acid solution from steel plants by coprecipitation. Then, the magnetic powder was added to a titanium sulfate solution and the hydroxides of titanium were precipitated at desired pH with urea solution. After filtration, drying, and grinding, the precipitates were sintered at 500°C under N_2 atmosphere to form the magnetic photocatalyst, Ni-Zn ferrite/TiO_2. The degradations of simulated FBL (Everdirect Supra Turquoise Blue) dye wastewater were carried out by applying self-prepared magnetic photocatalysts under UVA irradiation. Also L-H kinetic model was studied.

2. Materials and Methods

2.1. Preparation of Magnetic Ni-Zn Ferrite Powder and Magnetic Photocatalyst. Nitric acid was added sequentially to the small piece of lead frame scraps to dissolve nickel and iron. When hydrolysis was complete, tins were all precipitated as $Sn(OH)_4$ and the filtrate contained Ni^{+2} and Fe^{+2} ions. After detinning and according to the nickel concentration, waste acids from steel industry containing iron and reagent of zinc nitrate were added to the solution to adjust the solution composition as $Ni_{1-X}Zn_XFe_2O_4$, where X is chosen as 0.5. NaOH solution is then added to adjust the solution pH value to alkali. Subsequently, all Fe, Ni, and Zn ions in the solution were transformed into hydroxide forms and suspended in the solution. The solution was pumped with air to oxidize ferrous ion and heated for several hours. All hydroxides were reacted and precipitated from the solution as ferrite powders. Ni-Zn ferrite powders were filtered, washed, calcined, and dried. The designed composition was Ni : Zn : Fe = 0.5 : 0.5 : 2.0 by moles and Ni : Zn : Fe = 16.9 : 18.8 : 64.3 by weight percentages or NiO : ZnO : Fe_2O_3 = 9.4 : 10.2 : 80.4 by weight. Corresponding reactions are shown in the following:

$$5Sn + 4HNO_3 + 8H_2O \longrightarrow 5Sn(OH)_4 + 2N_2 \quad (1)$$

$$5(Fe, Ni) + 12HNO_3 \longrightarrow 5(Fe, Ni)(NO_3)_2 + N_2 + 6H_2O \quad (2)$$

$$Ni(NO_3)_{2(aq)} + Fe(NO_3)_{3(aq)} + Zn(NO_3)_{2(aq)} + 7NaOH_{(aq)} \longrightarrow Ni(OH)_2 + Fe(OH)_3 + Zn(OH)_2 + 7NaNO_3 \quad (3)$$

$$(1 - X)\,Ni(OH)_2 + 2Fe(OH)_3 + X\,Zn(OH)_2 \longrightarrow Ni_{1-X}Zn_XFe_2O_4 + 4H_2O \quad (4)$$

Experimental treatment with photocatalyst-TiO_2 alone for dye wastewater is proved to be very efficient. Besides, the secondary pollution by other advanced treatment methods can be eliminated. But there still exists the separation problem of solids (TiO_2) and liquids (wastewater). Therefore, used in this study were titanium sulfate, urea, and Ni-Zn ferrite powder to produce modified titanium dioxide photocatalyst by coprecipitation. The ratio of Ni-Zn ferrite powder to TiO_2 was 1 : 1 (wt%). Finally magnetic photocatalyst powder was obtained by filtration, drying, grinding, and calcination at 500°C. The same procedure was used for the preparation of TiO_2 except the step of no addition of magnetic Ni-Zn ferrite powder. Related reactions were

$$(NH_2)_2CO + 3H_2O \longrightarrow 2NH_4OH + CO_2 \quad (5)$$

$$Ti(SO_4)_2 + 4NH_4OH \longrightarrow Ti(OH)_4 + 2(NH_4)_2SO_4 \quad (6)$$

$$Ti(OH)_4 \longrightarrow TiO_2 + 2H_2O \quad (7)$$

The characterizations of the prepared Ni-Zn ferrite powders and modified magnetic photocatalysts, Ni-Zn ferrite/TiO_2, were investigated by ICP, XRF, XRD, SEM, SQUID, and BET measurements. TOC and ADMI values can be applied for the treatment of dye wastewater under UVA irradiation with the self-prepared TiO_2 and Ni-Zn ferrite/TiO_2 magnetic photocatalysts.

2.2. Characterization. The crystalline structures of both magnetic powder and magnetic photocatalyst were examined by XRD (X-ray diffractometer, XRD-6000, Shimadzu, Japan). Their M-H loops were measured by SQUID (superconducting quantum interference device, MPM57, Quantum Design, USA). Particle chemical compositions were analyzed by ICP (ICAP 9000, USA) and XRF (X-ray fluorescence, XEPOS/XEPO1, Spectro Co., Germany). Their microstructures were observed by SEM (scanning electron microscopy, S-3000N, Hitachi, Japan). The specific area was measured by BET surface area analyzer (Brunauer-Emmett-Teller, Model-ASAP 2012, Micromeritics, USA).

2.3. Photocatalytic Degradation. Photocatalytic reactions were carried out by mixing 1 L of FBL dye solution and 5 g of magnetic Ni-Zn ferrite/TiO_2 photocatalysts inside a 2 L

Table 1: Analysis of IC lead frame scraps by ICP.

Element	Fe	Ni	Sn
Concentration (ppm)	25325	18246	9571
Wt%	47.66%	34.33%	18.01%

Table 2: Analysis of filtrate after detinning by ICP.

Element	Fe	Ni
Concentration (ppm)	20364.75	14936.60
Weight %	57.69%	42.31%
Molarity (mole/L)	0.36	0.25

photoreactor with a Teflon agitator under UVA irradiation for 8 hrs. The structure of the FBL dye was shown in [8]. The initial dye concentrations were COD = 100, 200, 300, and 400 mg/L for each experiment. After photoreaction and filtration by 0.45 μm MFS, TOC (total organic carbon, Model 1010, O.I. Analytical, USA) and ADMI color values (American Dye Manufacturers Institute, Model DR/4000V, HACH, USA) were measured for each sample. COD was determined by potassium dichromate titration as described in Standard Methods [36]. UVA intensities were measured by a radiometer (Lutron Co., Taiwan) and expressed as I_{av} (mW/cm^2).

3. Results and Discussion

3.1. Characterization of Magnetic Photocatalyst of Ni-Zn Ferrite/TiO$_2$. The compositions of IC lead frame scraps and filtrate after detinning are shown in Tables 1 and 2, respectively.

XRF analyses of Ni-Zn ferrite powders and Ni-Zn ferrite/TiO$_2$ are shown in Table 3. It is clear that the experimental values of magnetic powders from wastes are close to the quantity of the predetermined value. SEM micrographs suggest that particles of magnetic Ni-Zn ferrite powders agglomerate. The particle size is around 0.3 μm by DLS (dynamic light scattering) analysis [37]. TiO$_2$ is precipitated on the surface of the secondary particle and its size is approximately 469.7 nm as shown in Figure 1. EDX diagrams of Ni-Zn ferrite powders and Ni-Zn ferrite/TiO$_2$ photocatalyst indicate the presence of Ni, Zn, Fe, and titanium as shown in Figure 2. X-ray diffraction patterns of Ni-Zn ferrite powders and magnetic photocatalysts in Figure 3 reveal the spinel cubic ferrites and the anatase form of TiO$_2$. All peaks in the pattern match well with the Joint Committee of Powder Diffraction Standard (JCDDS). A small amount of hematite also exists in the specimens. The surface area of Ni-Zn ferrite powder by BET measurement is 17 m^2/g and that of Ni-Zn ferrite/TiO$_2$ rises to 61 m^2/g, which shows more active sites for photoreaction.

The self-prepared TiO$_2$ follows the same coprecipitation without the addition of Ni-Zn ferrite powder and the corresponding SEM and EDX diagrams are shown in Figures 4 and 5. The particle size is around 1 μm–4.8 μm and BET is 116 (m^2/g) while BET of commercial TiO$_2$ (7 nm) is 231 (m^2/g).

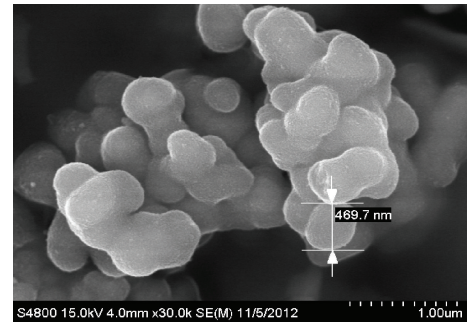

Figure 1: SEM diagram of Ni-Zn ferrite/TiO$_2$ (×30000).

3.2. Magnetic Property. Magnetic properties of Ni-Zn ferrite powders and Ni-Zn ferrite/TiO$_2$ are presented in Figure 6 as magnetic hysteresis loops by SQUID. The saturation magnetization (Ms) of Ni-Zn ferrite powder and Ni-Zn ferrite/TiO$_2$ is 64.43 and 17.05 emu/g and the corresponding coercive forces (Hc) are 6.13 and 7.66 Oe, respectively. Due to the minimal hysteresis and small Hc, the prepared magnetic materials are all soft magnetic and the magnetic photocatalysts made up from wastes can be recycled by applied magnetic field because of the magnetic property. The small coercivity of the ferrite mainly comes from the soft magnetic properties of the Ni-Zn ferrite, which has very low crystal and shape anisotropy constant, and is not due to size effect [38]. The saturation magnetization of the ferrite ($Ni_{0.5}Zn_{0.5}Fe_2O_4$) prepared here is 64.43 emu/g, and the literature values are about 70 emu/g [39], depending on the preparation conditions. They are quite comparable.

3.3. Photodegradation. Photodegradations of simulated FBL dye wastewater at initial CODs of 100, 200, 300, and 400 mg/L under UVA irradiation with self-produced magnetic photocatalysts from wastes are shown in Figures 7 and 8. The degradation efficiencies increase as the pollutant concentrations decrease. For dilute pollution of FBL dye (COD = 100 ppm), TOC removal can reach 84.22% and color or ADMI removal reaches 81.68%. The photodegradations by self-prepared TiO$_2$, commercial TiO$_2$, and Ni-Zn ferrite/TiO$_2$ are also summarized and compared in Table 4. Ni-Zn ferrite/TiO$_2$ from wastes is very close to the commercial TiO$_2$ (20 nm) in treatment efficiency by treating dilute simulated dye wastewater. The treatment efficiency of the self-prepared TiO$_2$ is better than that of the commercial TiO$_2$ (20 nm).

3.4. Langmuir-Hinshelwood Kinetic Model (L-H Model). L-H model can be expressed by the following equation:

$$r = -\frac{dC}{dt} = \frac{k_r KC}{1 + KC} = \frac{k_d C}{1 + KC}, \quad (8)$$

where k_r is the photocatalytic reaction constant [mg/(L-min)], k_d is the apparent degradation rate constant (min^{-1}), and C is the dye concentration, TOC (mg/L). Combining zero-order and first-order reactions, L-H model becomes [40]

$$-\ln\left(\frac{C}{C_0}\right) + K\left(C_0 - C\right) = K_r K t. \quad (9)$$

Table 3: XRF analysis of magnetic materials ($Ni_{0.5}Zn_{0.5}Fe_2O_4$ and Ni-Zn ferrite/TiO_2).

Items	Fe_2O_3 (wt%)	NiO (wt%)	ZnO (wt%)	TiO_2 (wt%)
$Ni_{0.5}Zn_{0.5}Fe_2O_4$ (designed value)	80.4 wt%	9.4 wt%	10.20 wt%	—
$Ni_{0.5}Zn_{0.5}Fe_2O_4$ (experimental)	79.71 wt%	9.5 wt%	10.78 wt%	—
Ni -Zn ferrite/TiO_2 (500°C) (experimental)	28.58 wt%	2.58 wt%	3.63 wt%	65.22 wt%

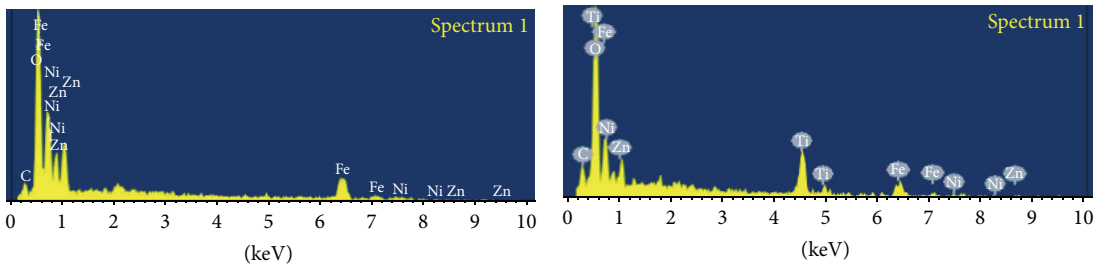

Figure 2: EDX of Ni-Zn ferrite powder (a) and Ni-Zn ferrite/TiO_2 (b).

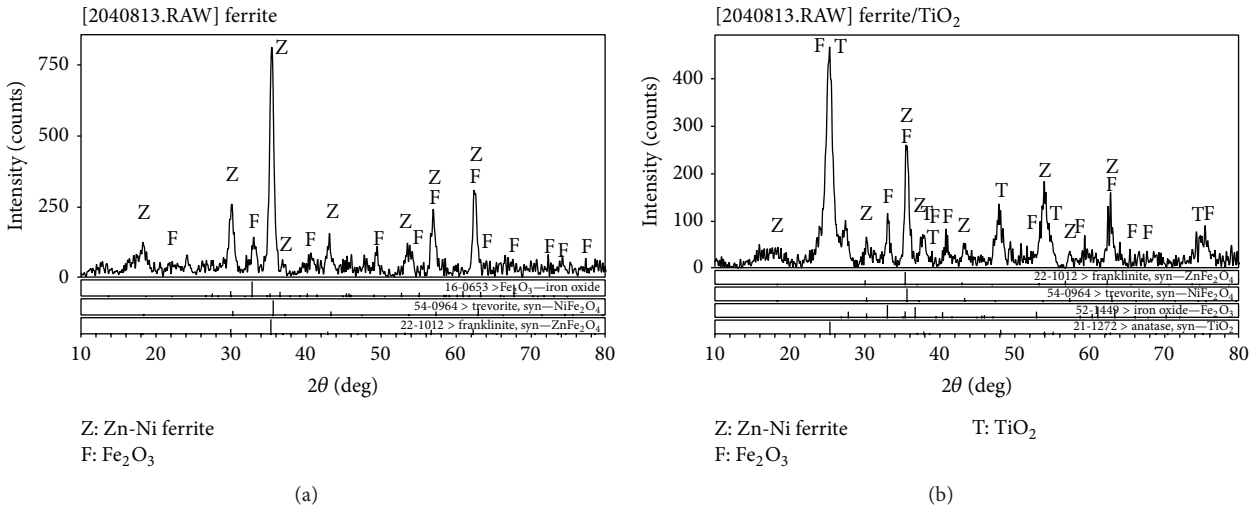

Figure 3: XRD diagram of Ni-Zn ferrite powder (a) and Ni-Zn ferrite/TiO_2 (500°C) (b).

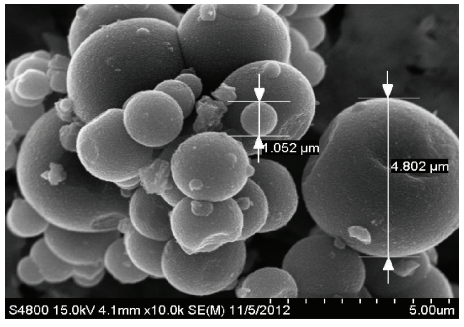

Figure 4: SEM images of self-prepared photocatalyst of TiO_2 (×10000).

Let $C = 0.715C_0$, $t = t_{0.715}$; the equation becomes

$$t_{0.715} = \frac{0.3354}{k_r K} + \frac{0.285C_0}{k_r}. \quad (10)$$

Plotting $t_{0.715}$ against $0.285C_0$ brings about a straight line as shown in Figure 9. From the slope and intercept, kinetic constants can be calculated.

Constants obtained from L-H model are k_r = 3.1614 (mg/L min), k_d = 0.3212 (min^{-1}), and $K = (k_d/k_r)$ = 0.1016 (L/mg). The result shows that L-H kinetic model fits well for the photodegradation of FBL simulated dye wastewater with the self-prepared Ni-Zn ferrite/TiO_2.

Table 4: Ultimate TOC and ADMI removal % of various TiO_2 (COD = 100 ppm, dosage = 5 g) under UVA irradiation (I_{av} = 1.324 W/cm^2).

Photocatalyst	Ni-Zn ferrite/TiO_2	Self-prepared TiO_2	Commercial TiO_2 (7 nm)	Commercial TiO_2 (20 nm)
TOC removal (%)	84.22%	91.71%	95.96%	84.40%
ADMI removal (%)	81.68%	93.04%	97.79%	87.66%

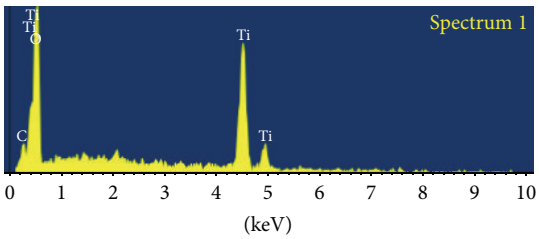

Figure 5: EDX of self-prepared photocatalyst of TiO_2.

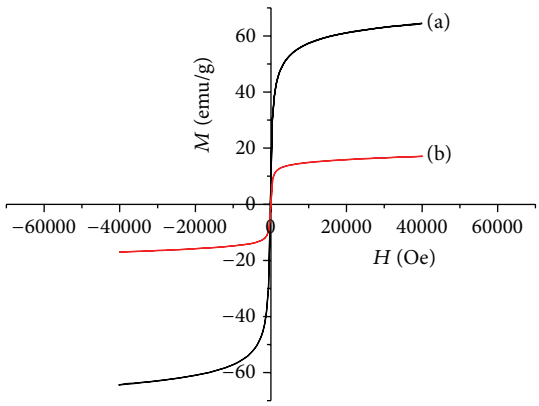

(a) Self-prepared Ni-Zn ferrite
(b) Ni-Zn ferrite/TiO_2

Figure 6: SQUID hysteresis loop of Ni-Zn ferrite powder and Ni-Zn ferrite/TiO_2 calcined at 500°C.

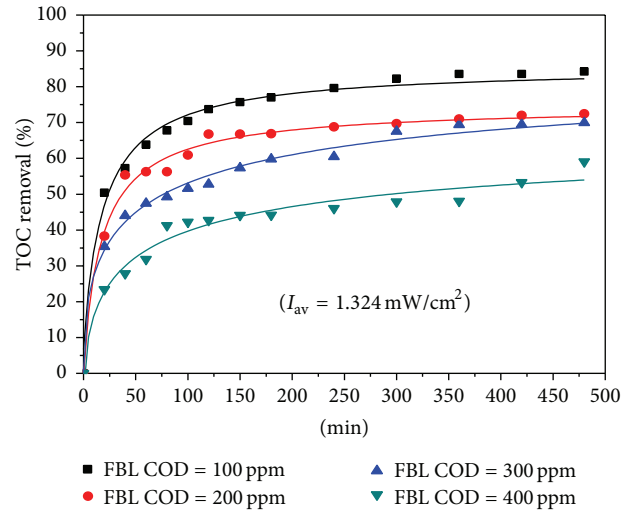

Figure 7: TOC removal % versus time with Ni-Zn ferrite/TiO_2 ($COD|_{t=0}$ = 100–400 ppm) to treat FBL dye (dosage = 5 g/L; I_{av} = 0.1324 mW/cm^2).

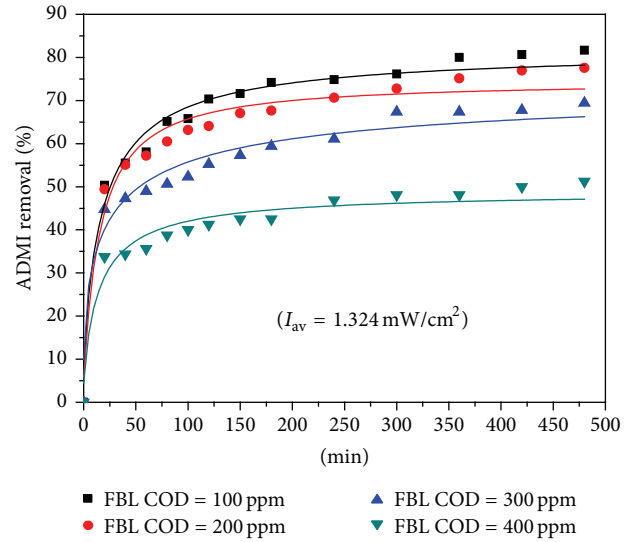

Figure 8: ADMI removal % versus time with Ni-Zn ferrite/TiO_2 ($COD|_{t=0}$ = 100–400 ppm) to treat FBL dye (dosage = 5 g/L; I_{av} = 0.1324 mW/cm^2).

4. Conclusions

The following conclusions can be drawn:

(1) Magnetic ferrite powder of $Ni_{0.5}$ $Zn_{0.5}Fe_2O_4$ was successfully prepared by coprecipitation from industrial wastes of IC lead frame and waste acids of steel industry.

(2) Magnetic photocatalyst of Ni-Zn ferrite/TiO_2 was also successfully fabricated from prepared magnetic ferrite powder, Ti $(SO_4)_2$, and urea by the same coprecipitation. By XRD analysis, TiO_2 in magnetic photocatalyst shows the crystal structure of anatase form.

(3) By SQUID analysis, the saturation magnetism (Ms) of the prepared magnetic photocatalysts is 17.05 emu/g with the coercive force (Hc) of 7.66 Oe, which proves that the magnetic photocatalyst is soft magnetic material and can be recycled by magnetic field.

(4) The degradation of FBL dye shows that TOC and ADMI removal efficiencies are quite close for the prepared Ni-Zn ferrite/TiO_2 and the commercial 20 (nm) TiO_2. The magnetic photocatalysts can solve the separation problem between wastewater and TiO_2 photocatalysts by magnetic field.

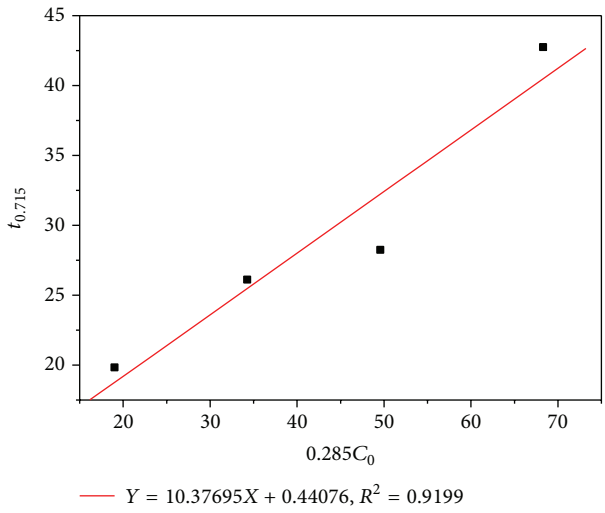

FIGURE 9: L-H kinetic model of magnetic photocatalysts of Ni-Zn ferrite/TiO_2.

(5) L-H kinetic model fits well for the self-prepared magnetic photocatalysts of Ni-Zn ferrite/TiO_2, which can be used successfully in AOP.

(6) Quite consequential is the transformation of hazardous wastes to valuable magnetic ferrite powders and magnetic photocatalysts and the processes studied not only recycle wastes to solve the global pollution problem but also tell the possibility of turning profits.

Conflict of Interests

The authors declare that there is no conflict of interests regarding the publication of this paper.

Acknowledgments

This project was supported by National Science Council, Taiwan, and Yeou Hung Material Technology Co., Ltd., Taiwan, under Contract no. NSC 100-2622-E-159-001-CC3. The authors express sincere gratitude for the financial support for this research.

References

[1] J. Pierce, "Colour in textile effluents, the origins of problems," *Journal of the Society of Dyers and Colourists*, vol. 110, pp. 131–133, 1994.

[2] I. Arslan, I. A. Balcioglu, T. Tuhkanen, and D. Bahnemann, "H_2O_2/UV-C and Fe^{2+}/H_2O_2/UV-C versus TiO_2/UV-A treatment for reactive dye wastewater," *Journal of Environmental Engineering*, vol. 126, no. 10, pp. 903–911, 2000.

[3] D. Tomova, V. Iliev, S. Rakovsky, M. Anachkov, A. Eliyas, and G. L. Puma, "Photocatalytic oxidation of 2,4,6-trinitrotoluene in the presence of ozone under irradiation with UV and visible light," *Journal of Photochemistry and Photobiology A: Chemistry*, vol. 231, no. 1, pp. 1–8, 2012.

[4] Y. Nakamura, F. Kobayashi, M. Daidai, and A. Kurosumi, "Purification of seawater contaminated with undegradable aromatic ring compounds using ozonolysis followed by titanium dioxide treatment," *Marine Pollution Bulletin*, vol. 57, no. 1–5, pp. 53–58, 2008.

[5] F. Fozzi, A. Machulek Jr., V. S. Ferreira et al., "Investigaton of chlorimuron-ethyl degradation by Fenton, photo-Fenton and ozonation processes," *Chemical Engineering Journal*, vol. 210, pp. 444–450, 2012.

[6] M. Karatas, Y. A. Argun, and M. E. Argun, "Decolorization of antraquinonic dye, Reactive Blue 114 from synthetic wastewater by Fenton process: kinetics and thermodynamics," *Journal of Industrial and Engineering Chemistry*, vol. 18, no. 3, pp. 1058–1062, 2012.

[7] S. Karthikeyan, A. Titus, A. Gnanamani, A. B. Mandal, and G. Sekaran, "Treatment of textile wastewater by homogeneous and heterogeneous Fenton oxidation processes," *Desalination*, vol. 281, no. 1, pp. 438–445, 2011.

[8] R. Liu, H. M. Chiu, C.-S. Shiau, R. Y.-L. Yeh, and Y.-T. Hung, "Degradation and sludge production of textile dyes by Fenton and photo-Fenton processes," *Dyes and Pigments*, vol. 73, no. 1, pp. 1–6, 2007.

[9] S. S. Abu Amr and H. A. Aziz, "New treatment of stabilized leachate by ozone/Fenton in the advanced oxidation process," *Waste Management*, vol. 32, no. 9, pp. 1693–1698, 2012.

[10] M. N. Chong, B. Jin, C. W. K. Chow, and C. Saint, "Recent developments in photocatalytic water treatment technology: a review," *Water Research*, vol. 44, no. 10, pp. 2997–3027, 2010.

[11] S. Bagwasi, B. Tian, J. Zhang, and M. Nasir, "Synthesis, characterization and application of bismuth and boron Co-doped TiO_2: a visible light active photocatalyst," *Chemical Engineering Journal*, vol. 217, pp. 108–118, 2013.

[12] M. Khraisheh, L. Wu, A. H. Al-Muhtaseb, A. B. Albadarin, and G. M. Walker, "Phenol degradation by powdered metal ion modified titanium dioxide photocatalysts," *Chemical Engineering Journal*, vol. 213, pp. 125–134, 2012.

[13] R. Liu, H. S. Wu, R. Yeh, C. Y. Lee, and Y. Hung, "Synthesis and bactericidal ability of TiO_2 and Ag-TiO_2 prepared by coprecipitation method," *International Journal of Photoenergy*, vol. 2012, Article ID 640487, 7 pages, 2012.

[14] A. Charanpahari, S. S. Umare, S. P. Gokhale, V. Sudarsan, B. Sreedhar, and R. Sasikala, "Enhanced photocatalytic activity of multi-doped TiO_2 for the degradation of methyl orange," *Applied Catalysis A: General*, vol. 443-444, pp. 96–102, 2012.

[15] Z.-D. Meng, F.-J. Zhang, L. Zhu et al., "Synthesis and characterization of M-fullerene/TiO_2 photocatalysts designed for degradation azo dye," *Materials Science and Engineering C*, vol. 32, no. 8, pp. 2175–2182, 2012.

[16] S. Yamazaki, Y. Fujiwara, S. Yabuno, K. Adachi, and K. Honda, "Synthesis of porous platinum-ion-doped titanium dioxide and the photocatalytic degradation of 4-chlorophenol under visible light irradiation," *Applied Catalysis B: Environmental*, vol. 121-122, pp. 148–153, 2012.

[17] B. Neppolian, A. Bruno, C. L. Bianchi, and M. Ashokkumar, "Graphene oxide based Pt-TiO_2 photocatalyst: ultrasound assisted synthesis, characterization and catalytic efficiency," *Ultrasonics Sonochemistry*, vol. 19, no. 1, pp. 9–15, 2012.

[18] S. R. Shirsath, D. V. Pinjari, P. R. Gogate, S. H. Sonawane, and A. B. Pandit, "Ultrasound assisted synthesis of doped TiO_2 nanoparticles: characterization and comparison of effectiveness for photocatalytic oxidation of dyestuff effluent," *Ultrasonics Sonochemistry*, vol. 20, no. 1, pp. 277–286, 2013.

[19] S. Chakma and V. S. Moholkar, "Physical mechanism of sono-fenton process," *AIChE Journal*, vol. 59, no. 11, pp. 4303–4313, 2013.

[20] S. Chakma and V. S. Moholkar, "Investigations in synergism of hybrid advanced oxidation processes with combinations of sonolysis + fenton process + UV for degradation of bisphenol A," *Industrial and Engineering Chemistry Research*, vol. 53, no. 16, pp. 6855–6865, 2014.

[21] J. Hu, M. Yan, and W. Luo, "Preparation of high-permeability NiZn ferrites at low sintering temperatures," *Physica B: Condensed Matter*, vol. 368, no. 1–4, pp. 251–260, 2005.

[22] H. Su, H. Zhang, X. Tang, Y. Jing, and Y. Liu, "Effects of composition and sintering temperature on properties of NiZn and NiCuZn ferrites," *Journal of Magnetism and Magnetic Materials*, vol. 310, no. 1, pp. 17–21, 2007.

[23] X. He, Q. Zhang, and Z. Ling, "Kinetics and magnetic properties of sol-gel derived NiZn ferrite-SiO_2 composites," *Materials Letters*, vol. 57, no. 20, pp. 3031–3036, 2003.

[24] H. H. He, G. S. Song, and J. H. Zhu, "Non-stoichiometric NiZn ferrite by sol-gel processing," *Materials Letters*, vol. 59, pp. 1941–1944, 2005.

[25] W.-C. Hsu, S. C. Chen, P. C. Kuo, C. T. Lie, and W. S. Tsai, "Preparation of NiCuZn ferrite nanoparticles from chemical co-precipitation method and the magnetic properties after sintering," *Materials Science and Engineering B*, vol. 111, no. 2-3, pp. 142–149, 2004.

[26] K. H. Wu, Y. M. Shin, C. C. Yang, G. P. Wang, and D. N. Horng, "Preparation and characterization of bamboo charcoal/$Ni_{0.5}Zn_{0.5}Fe_2O_4$ composite with core-shell structure," *Materials Letters*, vol. 60, no. 21-22, pp. 2707–2710, 2006.

[27] S. Verma, P. A. Joy, Y. B. Khollam, H. S. Potdar, and S. B. Deshpande, "Synthesis of nanosized $MgFe_2O_4$ powders by microwave hydrothermal method," *Materials Letters*, vol. 58, no. 6, pp. 1092–1095, 2004.

[28] A. Verma, T. C. Goel, R. G. Mendiratta, and R. G. Gupta, "High-resistivity nickel-zinc ferrites by the citrate precursor method," *Journal of Magnetism and Magnetic Materials*, vol. 192, no. 2, pp. 271–276, 1999.

[29] S. Deka and P. A. Joy, "Characterization of nanosized NiZn ferrite powders synthesized by an autocombustion method," *Materials Chemistry and Physics*, vol. 100, no. 1, pp. 98–101, 2006.

[30] K. H. Wu, Y. C. Chang, and G. P. Wang, "Preparation of NiZn ferrite/SiO_2 nanocomposite powders by sol-gel auto-combustion method," *Journal of Magnetism and Magnetic Materials*, vol. 269, no. 2, pp. 150–155, 2004.

[31] P. P. Goswami, H. A. Choudhury, S. Chakma, and V. S. Moholkar, "Sonochemical synthesis and characterization of manganese ferrite nanoparticles," *Industrial & Engineering Chemistry Research*, vol. 52, no. 50, pp. 17848–17855, 2013.

[32] F. Chen and J. Zhao, "Preparation and photocatalytic properties of a novel kind of loaded photocatalyst of $TiO_2/SiO_2/\gamma$-Fe_2O_3," *Catalysis Letters*, vol. 58, no. 4, pp. 246–247, 1999.

[33] Y. Gao, B. Chen, H. Li, and Y. Ma, "Preparation and characterization of a magnetically separated photocatalyst and its catalytic properties," *Materials Chemistry and Physics*, vol. 80, no. 1, pp. 348–355, 2003.

[34] Y.-P. Fu, W.-K. Chang, H.-C. Wang, C.-W. Liu, and C.-H. Lin, "Synthesis and characterization of anatase TiO_2 nanolayer coating on Ni-Cu-Zn ferrite powders for magnetic photocatalyst," *Journal of Materials Research*, vol. 25, no. 1, pp. 134–140, 2010.

[35] R. Liu, C. F. Wu, and M. D. Ger, "Degradation of FBL dye wastewater by magnetic photocatalysts from scraps," *Journal of Nanomaterials*, vol. 2015, Article ID 651021, 9 pages, 2015.

[36] APHA, *Standard Methods for the Examination of Water and Wastewater*, American Public Health Association, American Water Works Association, Water Environment Federation, Washington, DC, USA, 22nd edition, 2012.

[37] C. F. Wu, *Preparation, characterization and application of Mn-Zn ferrite powders and magnetic titanium dioxide from used dry batteries and spent steel pickling liquids [M.S. thesis]*, Department of Chemical and Materials Engineering, Minghsin University of Science and Technology, Hsinchu, Taiwan, 2012.

[38] B. D. Cullity and C. D. Graham, *Introduction to Magnetic Materials*, John Wiley & Sons, 2009.

[39] A. Goldman, *Modern Ferrite Technology*, Van Nostrand Reinhold, 1990.

[40] I. A. Alaton and I. A. Balcioglu, "Photochemical and heterogeneous photocatalytic degradation of waste vinylsulphone dyes: a case study with hydrolyzed Reactive Black 5," *Journal of Photochemistry and Photobiology A: Chemistry*, vol. 141, no. 2-3, pp. 247–254, 2001.